Available online at www.sciencedirect.com
ScienceDirect
International Journal of Mass Spectrometry 263 (2007) 12–21
International Journal of Mass Spectrometry
www.elsevier.com/locate/ijms

Detection of C_1–C_5 alkyl nitrates by proton transfer reaction time-of-flight mass spectrometry

Nobuyuki Aoki [1], Satoshi Inomata *, Hiroshi Tanimoto

Atmospheric Environment Division, National Institute for Environmental Studies, 16-2 Onogawa, Tsukuba, Ibaraki 305-8506, Japan

Received 6 September 2006; received in revised form 27 November 2006; accepted 27 November 2006
Available online 29 December 2006

Abstract

Characteristics of the mass spectra of C_1–C_5 alkyl nitrates ($RONO_2$) were systematically examined with a proton transfer reaction time-of-flight mass spectrometer operated at field strengths, *E*/*N*, of the drift tube of between 96 and 147 Td. Although protonated alkyl nitrates were detected for C_1–C_4 alkyl nitrates, their signal intensities were, at most, a few percent of the total ion signals. The major product ions were several fragment ions including NO_2^+, RO^+, R^+, and $ROH{\cdot}H^+$, the abundances and relative intensities of which depended on the *E*/*N* ratio. The intensity of NO_2^+ ions increased with increasing *E*/*N* ratio, whereas the intensities of organic fragments such as R^+ and RO^+ ions, relative to the total product ions, decreased with increasing *E*/*N* ratio. Those organic fragment ions partly underwent further fragmentation at high *E*/*N* ratios to produce $[R-2H]^+$, $[R-4H]^+$, and $[RO-2H]^+$, particularly for the higher alkyl nitrates. The fragmentation patterns also varied for the C_1–C_5 alkyl nitrates, the most predominant ions being the NO_2^+ for C_1–C_2 alkyl nitrates and R^+ ions for C_3–C_5 alkyl nitrates. Although the experimental finding that NO_2^+ fragment ions were detected regardless the speciation of alkyl nitrates suggested that the detection of C_1–C_2 alkyl nitrates by this technique is not selective, the abundant fragment ion signals of R^+ ions could be useful for the identification of C_3–C_5 alkyl nitrates.

Keywords: Proton transfer reaction; Time-of-flight mass spectrometry; PTR-MS; Alkyl nitrate

1. Introduction

Proton transfer reaction mass spectrometry (PTR-MS) is a technique that enables us to perform rapid analyses of volatile organic compounds (VOCs) with low detection limits [1–3]. Because PTR ionization is a soft ionization method that predominantly produces protonated molecules, PTR-MS is used in many branches of atmospheric chemistry research, including air-quality monitoring [4–7], flux measurements [8–11], and photooxidation studies [12–14]. The PTR-MS technique provides only information on the mass-to-charge ratio, *m*/*z*, of ions produced by PTR ionization. This sometimes complicates the assignment of the ion signals, and requires a careful identification of the chemical species involved [15].

Organic nitrates are produced in sequential oxidation processes of non-methane hydrocarbons (NMHCs) in the presence of nitrogen oxides (NO_x) [16]. It has been reported that the concentration of peroxyacetyl nitrate [$CH_3C(O)OONO_2$; PAN] in urban areas reaches maximum levels of the order or 10 parts per billion by volume (ppbv). The detection of peroxyacyl nitrates ($RC(O)OONO_2$), including PAN, peroxypropionic nitrate ($CH_3CH_2C(O)OONO_2$; PPN), and peroxymethacrylic nitrate ($CH_2{=}C(CH_3)C(O)OONO_2$; MPAN) by PTR-MS was reported by Hansel and Wisthaler [17]. They suggested that a protonated peroxyacyl nitrate, $RC(O)OONO_2{\cdot}H^+$, undergoes subsequent reactions with water vapor as a reagent gas to form the corresponding protonated organic peroxy acid ($RC(O)OOH{\cdot}H^+$) and nitric acid:

$$RC(O)OONO_2{\cdot}H^+ + H_2O \rightarrow RC(O)OOH{\cdot}H^+ + HNO_3 \quad (1)$$

The real-time detection of PAN, PPN, and MPAN in ambient air was demonstrated by monitoring, not the protonated peroxyacyl nitrate signals, but the ion signals at *m*/*z* 77 ($CH_3C(O)OOH{\cdot}H^+$), *m*/*z* 91 ($CH_3CH_2C(O)OOH{\cdot}H^+$), and *m*/*z* 103 ($CH_2{=}C(CH_3)C(O)OOH{\cdot}H^+$), respectively. As these ion

* Corresponding author. Tel.: +81 29 850 2403; fax: +81 29 850 2579.
E-mail address: ino@nies.go.jp (S. Inomata).
[1] Present address: National Metrology Institute of Japan, National Institute of Advanced Industrial Science and Technology, 1-1-1 Umezono, Tsukuba, Ibaraki 305-8563, Japan.

1387-3806/$ – see front matter © 2006 Elsevier B.V. All rights reserved.
doi:10.1016/j.ijms.2006.11.018

signals decreased when the sample air was passed through a heated tube at 120 °C, the difference in the ion signals was attributed to signals from the peroxyacyl nitrates [17].

Like peroxyacyl nitrates, alkyl nitrates ($RONO_2$) are formed by degradation and photooxidation of VOCs in air [16,18]. Although yields of alkyl nitrates are relatively low [16], the sum of their mixing ratios can be in the ppbv range in polluted air masses [19]. Recently, D'Anna et al. [12] reported that *n*-propyl nitrate and *n*-butyl nitrate (M) give weak (<1%) signals for the protonated alkyl nitrate (MH^+) with PTR-MS detection and they found that $[MH - HNO_3]^+$ ions were predominantly produced with minor amounts of $[MH + H_2O - HNO_3]^+$, $[MH - HNO_2]^+$, NO_2^+, and fragment ions of the carbon skeleton. The product ions, their relative signal abundances, and their sensitivities were determined in the case of *n*-butyl nitrate only: the characteristics and patterns of mass spectra of other alkyl nitrates were not reported.

In the present work, the mass spectra of seven C_1–C_5 alkyl nitrates, including *n*-alkyl nitrates and isoalkyl nitrates, were investigated by using a proton transfer reaction time-of-flight mass spectrometer (PTR-TOFMS), recently developed in our laboratory [20,21]. To explore the possibility of detecting alkyl nitrates in real-time by using PTR-MS instruments, a better characterization of the mass spectra and fragmentation patterns of alkyl nitrates is required. In this paper, we present speciation of the product ions of C_1–C_5 alkyl nitrates obtained by PTR ionization and we provide rough estimates of the detection sensitivity compared with that of a typical VOC. The results will be useful in evaluating possible interference from alkyl nitrates in both field measurements and smog-chamber experiments when using PTR-MS instruments.

2. Experimental

2.1. Apparatus

The instrument used in the present work had a hollow-cathode ion source coupled through a drift tube to an orthogonal time-of-flight mass spectrometer. The detailed instrumental setup has been described elsewhere [20,21]. Briefly, the combination of an ion source and drift tube consisted of seven stainless-steel electrodes (ED1–ED7), an inlet lens (IL), and an orifice plate (OP) separated by static dissipative Teflon cylinders (Semitron ESD500, Nippon Polypenco). Adjoining electrodes were connected by resistances, and high positive voltages were applied to the electrodes from ED1 to ED7 by a common direct current (dc) power supply (HAR-5R6, Matsusada Precision Inc.). The voltages of the IL and the OP were controlled independently.

Water taken from the vapor pressure over distilled water (Wako Chemicals) was directed into the ion source as a reagent gas. Reagent ions (H_3O^+) and a small amount of $H_3O^+\cdot(H_2O)_{n=1,2}$ clusters, generated in the ion source, were introduced into the drift tube and react with VOCs in sample gases that were introduced from a sampling port located beneath the ion-source region. The pressure of the drift tube was maintained at 5 Torr. The product ions from the proton transfer reaction, together with residual reagent ions, were ejected into an ion-transfer region through a small orifice in a small-aperture disk (i.d. ~400 μm, thickness 50 μm, diameter 9.5 mm, stainless-steel, Lenox Laser) attached to the OP. The outgoing ions were transported through a skimmer, focused into a narrow beam by an einzel lens, and directed to the pulse-extraction electrodes of the two-stage accelerator. The ions were then extracted into the field-free flight region (50 cm long, single-path) perpendicularly to the ion beam transported from the drift tube. A dual multi-channel plate (MCP, TOF-2003, Burle) detector was used for ion detection. Ion signals were transferred to a time-to-digital converter (TDC, P7887, Fast ComTec) with 2 ns time bins, where the ion signals were discriminated, counted, and integrated during 100 s at a repetition of 10 kHz (i.e., 1×10^6 scans).

Mass spectra of alkyl nitrates were investigated at three *E*/*N* conditions of the drift tube: 96, 122, and 147 Td, where *E* is the electric field strength (V cm^{-1}), *N* is the buffer gas number density (molecule cm^{-3}), and 1 Td = 10^{-17} cm^2 V molecule^{-1}. These values correspond to the lowest *E*/*N* ratio in our system and the minimum and maximum values of typical *E*/*N* ratios in standard PTR-MS operation [1], respectively. Typical intensities of H_3O^+, $H_3O^+\cdot H_2O$, $H_3O^+\cdot(H_2O)_2$, and O_2^+ ions were 2.8×10^6, 6.3×10^5, 4.0×10^4, and 1.5×10^2 counts, respectively, at *E*/*N* = 96 Td. The corresponding values at *E*/*N* = 122 Td were 2.8×10^6, 5.3×10^5, 2.5×10^4, and 3.7×10^3 counts, respectively. At *E*/*N* = 147 Td, they were 4.0×10^6, 4.2×10^5, 1.5×10^4, and 2.6×10^4 counts, respectively. The intensities of other background signals were less than 1% of those of H_3O^+ ions.

2.2. Preparation of alkyl nitrates

Methyl nitrate was synthesized by the reaction of methanol, with a mixture of concentrated nitric and sulfuric acids (1:1) [22]. Ethyl, *n*-propyl, *n*-butyl, and *n*-pentyl nitrates were synthesized by the reaction of the corresponding *n*-alkyl bromides with silver nitrate dissolved in acetonitrile [23]. These alkyl nitrates were extracted with dichloromethane and then purified by vacuum distillation. All chemicals used in the syntheses were reagent grade: nitric acid (69–70%), methanol (>98%), ethyl bromide (>98%), *n*-propyl bromide (>97%), *n*-butyl bromide (>95%), *n*-pentyl bromide (>97%), silver nitrate (>99.8%), and acetonitrile (>99.5%) were from Wako Chemicals; sulfuric acid (>96%) and dichloromethane (>99%) were from Kanto Kagaku. Because the boiling point of acetonitrile is 81.6 °C, which is relatively close to those of the ethyl, *n*-propyl, *n*-butyl, and *n*-pentyl nitrates (87.2–157 °C) [16,24], large amounts of acetonitrile as an impurity were present in the synthesized samples of these nitrates: the amounts of acetonitrile were estimated to be approximately 75%, 70%, 50%, and 50% in ethyl, *n*-propyl, *n*-butyl, and *n*-pentyl nitrate samples, respectively. The fraction of impurity was determined by comparing the ion signals of protonated acetonitrile obtained from a pure sample of acetonitrile with those obtained from the synthesized *n*-alkyl nitrate samples, assuming that all the injected liquids evaporated. Isopropyl nitrate (>99%) and isobutyl nitrate (>96%) were purchased from Acros Organics and Aldrich Chem. Co., respectively.

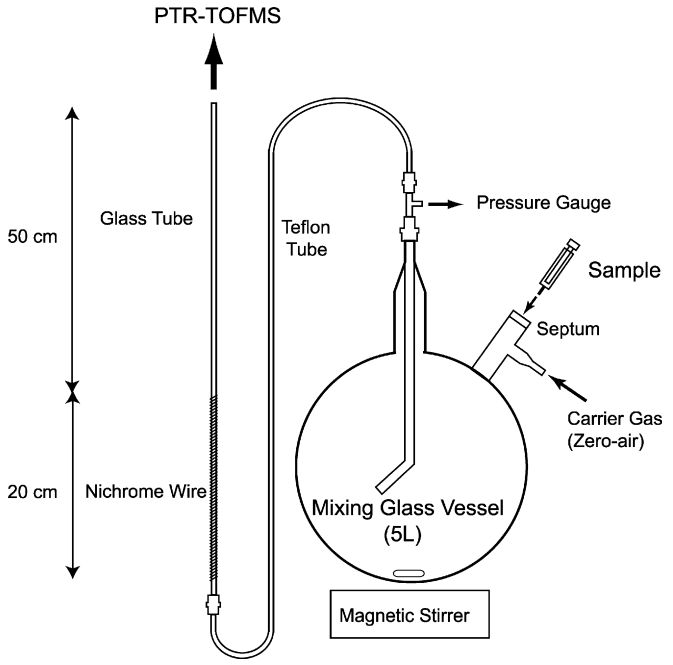

Fig. 1. Schematic showing the experimental setup. A sample inlet, a mixing vessel (5 L), and a thermal decomposition tube are shown. A liquid sample of 0.1 μL is injected into the mixing vessel with a syringe. The glass tube can be heated to 250 °C.

The proton affinities (PAs) of methyl nitrate, ethyl nitrate, and acetonitrile have been reported to be 734, 746, and 779 kJ mol^{-1}, respectively, which are greater than that of H_2O (691 kJ mol^{-1}) [24,25]. Although the PAs of other alkyl nitrates have not been reported, it is expected that they will be larger than that of ethyl nitrate, because PAs generally increase with increasing numbers of carbon atoms (C_n) for alkanes, alkenes, alcohols, etc. [24].

2.3. Sample inlet, mixing vessel, and thermal decomposition tube

Fig. 1 shows a 5 L mixing Pyrex glass vessel into which liquid samples were injected by a syringe then vaporized and diluted with air from a zero-air supply (Model 111, Thermo Environmental Instruments Inc.). Gases in the vessel were well mixed by using a magnetic stirrer. A small amount of each sample (0.1 μL) was injected into the vessel, resulting in a sample mixture of approximately 5 parts per million by volume (ppmv). An outlet of the vessel was connected to a Pyrex glass tube (70 cm long, o.d. 6 mm) by a 0.25 in. PFA tube. An upstream region of the glass tube (about 20 cm long) could be heated by a coiled nichrome wire (California Fine Wire Co.) at 250 °C to decompose the alkyl nitrates. The residence time of gas samples in the heated region was approximately 0.4 s. One end of the glass tube was connected to the inlet of the PTR-TOFMS instrument by a 0.25 in. PFA tube. After each measurement, we repeatedly cleaned the vessel by evacuating and purging with zero-air to flush any residuals from VOCs. The mass spectrum of acetonitrile, which gives a single peak of $CH_3CN{\cdot}H^+$ at m/z 42, was measured as a reference under each set of different experimental conditions.

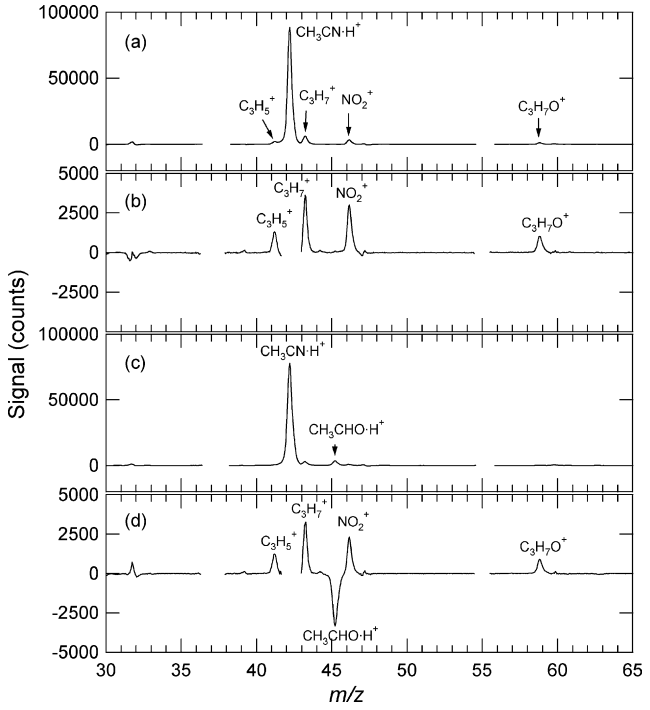

Fig. 2. (a) Mass spectrum of the *n*-propyl nitrate sample at $E/N = 122$ Td. (b) Mass spectrum of the reference sample is subtracted from (a). (c) Mass spectrum of thermally decomposed sample. (d) (a)–(c).

3. Results

3.1. Thermal decomposition of alkyl nitrates

The mass spectrum of a sample of *n*-propyl nitrate is shown in Fig. 2a. In this mass spectrum, ion signals at m/z 37 ($H_3O^+H_2O$) and m/z 55 ($H_3O^+(H_2O)_2$) are masked because these ion signals are largely scattered as a result of the subtraction of the background mass spectrum. Strong ion signals of protonated acetonitrile resulting from the presence of acetonitrile as an impurity in the sample were observed at m/z 42. Fig. 2b shows the mass spectrum of *n*-propyl nitrate when the reference mass spectrum of acetonitrile is subtracted. Residual ion signals found at m/z 41, 43, 46, and 59 were attributed to $C_3H_5^+$, $C_3H_7^+$, NO_2^+, and $C_3H_7O^+$, respectively: in addition, ion signals of protonated *n*-propyl nitrates were observed at m/z 106 (see Section 3.4). To verify that these ion signals originated from *n*-propyl nitrate, the sample was passed through a thermal decomposition tube heated to 250 °C. The *n*-propyl nitrate thermally decomposes to $CH_3CH_2CH_2O$ and NO_2 [26,27] whereas acetonitrile does not decompose.

$$CH_3CH_2CH_2ONO_2 \rightarrow CH_3CH_2CH_2O + NO_2 \quad (2)$$

The mass spectrum obtained when the sample was passed through the heated tube is shown in Fig. 2c. The ion intensity of acetonitrile at m/z 42 was as great as that observed in Fig. 2a, whereas the ion signals at m/z 41, 43, 46, and 59 were considerably decreased. Fig. 2d shows the difference between the mass spectrum of the *n*-propyl nitrate sample (Fig. 2a) and that of the thermally decomposed sample (Fig. 2c). The mass spectrum in

Fig. 2d is quite similar to that in Fig. 2b: indeed, the ratios of the ion signals at *m/z* 41, 43, 46, and 59 are 0.36:1.00:0.83:0.29 in Fig. 2b and 0.38:1.00:0.71:0.27 in Fig. 2d.

The fact that the ion intensity at around *m/z* 45 was negative in Fig. 2d indicates that some chemical species was produced by thermal decomposition of *n*-propyl nitrate at 250 °C. This ion is probably protonated acetaldehyde, $CH_3CHO{\cdot}H^+$, because acetaldehyde should be formed by the sequential reactions of the thermally decomposed *n*-propyl nitrate (reaction (2)) as follows:

$$CH_3CH_2CH_2O + M \rightarrow C_2H_5 + H_2CO + M \quad (3)$$

$$C_2H_5 + O_2 + M \rightarrow C_2H_5O_2 + M \quad (4)$$

$$2C_2H_5O_2 \rightarrow 2C_2H_5O + O_2 \quad (5)$$

$$C_2H_5O + O_2 \rightarrow CH_3CHO + HO_2 \quad (6)$$

The thermal decomposition of $CH_3CH_2CH_2O$ (reaction (3)) competes with the reaction of the alkoxy radicals with O_2; however, the decay rate (k') of the thermal decomposition of the $CH_3CH_2CH_2O$ at 250 °C ($k' \approx 5 \times 10^7\ s^{-1}$) [28] is estimated to be much faster than that of $CH_3CH_2CH_2O$ by reaction with O_2 ($k' \approx 4 \times 10^4\ s^{-1}$) [29]. Another product, H_2CO, in reaction (3) is stable, but was not detected here.

Consequently, we discuss the characteristics of the mass spectra of ethyl, *n*-propyl, *n*-butyl, and *n*-pentyl nitrates based on the mass spectra obtained by subtracting reference acetonitrile spectra from the sample spectra, because the thermal decomposition of these alkyl nitrates may produce organic species and interfere with the mass spectra. For the mass spectra of methyl, isopropyl, and isobutyl nitrates, the mass spectra obtained merely by subtracting the background mass spectra from the sample mass spectra are used for discussion.

3.2. Mass spectrum of methyl nitrate

Mass spectra of methyl nitrate at three different *E/N* conditions are shown in Fig. 3. Ion signals of the protonated methyl nitrate ($M_m{\cdot}H^+$) can be observed at *m/z* 78 at all *E/N* conditions.

$$CH_3ONO_2 + H_3O^+ \rightarrow M_m{\cdot}H^+ + H_2O,\ \Delta H^\circ_{rxn} = -43\ kJ\ mol^{-1} \quad (7a)$$

This peak is, however, very weak at each *E/N* ratio and the strongest ion signals were observed at *m/z* 46, attributed to NO_2^+. If NO_2^+ is produced directly by the reaction of CH_3ONO_2 with H_3O^+, the channel producing NO_2^+, CH_3OH, and H_2O (reaction (7b)) appears to be the lowest path energetically. This reaction is, however, expected to be endothermic ($\Delta H^\circ_{rxn} = +40\ kJ\ mol^{-1}$) [24].

$$CH_3ONO_2 + H_3O^+ \rightarrow NO_2^+ + CH_3OH + H_2O \quad (7b)$$

Because the mean relative center-of-mass kinetic energies, KE_{cm} [1], for the reactions of methyl nitrate with H_3O^+ are estimated to be 13, 20, and 27 kJ mol^{-1} at *E/N* = 96, 122, and 147 Td, respectively, the direct formation of the NO_2^+ ions by the two-body reaction (7b) would seem to be energetically unfavorable. It has been proposed that the lowest energy form of the protonated methyl nitrate is a complex between CH_3OH and NO_2^+, i.e. $CH_3OH{\cdot}NO_2^+$, rather than $CH_3ONO_2{\cdot}H^+$ [30,31]. The binding energy (BE) of this complex was estimated to be about 80 kJ mol^{-1} [30,32]. This BE is quite low, so that the $CH_3OH{\cdot}NO_2^+$ formed would easily decompose to CH_3OH and NO_2^+ by collisions (collision-induced dissociation, CID).

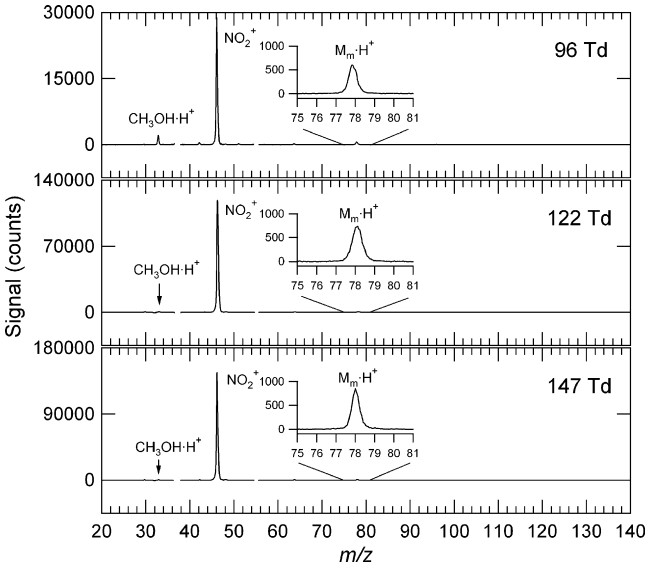

Fig. 3. Mass spectra of methyl nitrate at three different *E/N* conditions.

$$CH_3ONO_2 + H_3O^+ \rightarrow CH_3OH{\cdot}NO_2^+ + H_2O \quad (7a')$$

$$CH_3OH{\cdot}NO_2^+ \rightarrow CH_3OH + NO_2^+ \quad (8)$$

Indeed, the fractional contribution of NO_2^+ signals increases and that of $M_m{\cdot}H^+$ decreases with the increasing *E/N* ratio, as shown in Table 1.

Small ion signals observed at *m/z* 33 are assigned to $CH_3OH{\cdot}H^+$. The $CH_3OH{\cdot}H^+$ ions are not formed by the PTR ionization of methanol in the methyl nitrate sample as an impurity, because the signal ratios of *m/z* 33 ($CH_3OH{\cdot}H^+$) to *m/z* 46 (NO_2^+) decrease with increasing *E/N* ratio. The $CH_3OH{\cdot}H^+$ could be produced along with HNO_3 in the reaction of CH_3ONO_2 with H_3O^+, for which the ΔH°_{rxn} is estimated to be −34 kJ mol^{-1} [24].

$$CH_3ONO_2 + H_3O^+ \rightarrow CH_3OH{\cdot}H^+ + HNO_3 \quad (7c)$$

However, this reaction could not compete with reaction (7a) because reaction (7c) would require considerable rearrangement, which proceeds via a high-energy transition state. Possible processes for the formation of $CH_3OH{\cdot}H^+$ involve reactions of CH_3ONO_2 with $H_3O^+{\cdot}(H_2O)_{n=1,2}$ clusters.

$$CH_3ONO_2 + H_3O^+{\cdot}(H_2O)_{n=1,2} \rightarrow CH_3OH{\cdot}H^+ + HNO_3 + nH_2O \quad (9)$$

The decrease in the ratio of the signals at *m/z* 33 ($CH_3OH{\cdot}H^+$) and *m/z* 46 (NO_2^+) with increasing *E/N* ratio can be explained by the decrease in the intensities of $H_3O^+{\cdot}(H_2O)_{n=1,2}$ clusters relative to that of H_3O^+.

Table 1
Summary of product ions and their fractional contribution to the total ion signals obtained under three different *E*/*N* conditions

Alkyl nitrates	Product ions	*m*/*z*	Relative intensity		
			96 Td	122 Td	147 Td
CH_3ONO_2	$M_m{\cdot}H^+$	78	2.0	0.7	0.5
	NO_2^+	46	90.6	98.6	99.1
	$CH_3OH{\cdot}H^+$	33	7.4	0.7	0.4
$C_2H_5ONO_2$	$M_e{\cdot}H^+$	92	1.2	0.3	0.2
	NO_2^+	46	72.1	92.9	96.6
	$C_2H_5O^+$	45	14.1	5.0	3.2
	$C_2H_5OH{\cdot}H^+$	47	12.6	1.8	0.0
n-$C_3H_7ONO_2$	$M_{pr}{\cdot}H^+$	106	0.3	0.3	0.2
	NO_2^+	46	20.5	29.5	42.7
	$C_3H_7^+$	43	67.0	39.4	16.8
	$C_3H_5^+$	41	7.7	16.2	14.0
	$C_3H_7O^+$	59	4.5	14.6	5.5
	$C_3H_3^+$	39	–	–	19.7
	$C_3H_5O^+$	57	–	–	1.1
i-$C_3H_7ONO_2$	$M_{pr}{\cdot}H^+$	106	0.5	0.2	0.2
	NO_2^+	46	2.9	8.2	11.9
	$C_3H_7^+$	43	83.1	65.2	27.0
	$C_3H_5^+$	41	13.5	20.0	21.6
	$C_3H_7O^+$	59	∼0	6.4	2.7
	$C_3H_3^+$	39	–	–	33.6
	$C_3H_5O^+$	57	–	–	3.0
n-$C_4H_9ONO_2$	$M_b{\cdot}H^+$	106	∼0	∼0	∼0
	NO_2^+	46	6.8	7.2	8.4
	$C_4H_9^+$	57	92.0	92.2	58.3
	$C_4H_9O^+$	73	1.2	0.6	0.9
	$C_3H_5^+$	41	–	–	10.3
	$C_3H_3^+$	39	–	–	22.1
i-$C_4H_9ONO_2$	$M_b{\cdot}H^+$	120	0.1	0.1	0.1
	NO_2^+	46	0.9	3.9	8.5
	$C_4H_9^+$	57	85.6	73.9	44.9
	$C_4H_9O^+$	73	3.5	12.3	18.3
	$C_3H_7O^+$	59	7.2	5.0	6.6
	$C_3H_5^+$	41	2.7	4.8	9.5
	$C_3H_3^+$	39	–	–	12.1
n-$C_5H_{11}ONO_2$	NO_2^+	46	3.3	3.4	8.5
	$C_5H_{11}^+$	71	74.0	47.7	21.4
	$C_5H_9^+$	69	3.2	11.8	5.4
	$C_2H_5O^+$	45	8.6	6.0	8.2
	$C_3H_7^+$	43	10.9	24.5	11.4
	$C_3H_5^+$	41	–	6.6	13.1
	$C_3H_3^+$	39	–	–	32.0

3.3. Mass spectrum of ethyl nitrate

Mass spectra of ethyl nitrate are shown in Fig. 4. Like the mass spectra of methyl nitrate, ion signals of protonated ethyl nitrate ($M_e{\cdot}H^+$), NO_2^+, and $C_2H_5OH{\cdot}H^+$ are observed at *m*/*z* 92, 46, and 47, respectively, and the strongest peak is that of NO_2^+. Because the dependence of the fractional contributions of $M_e{\cdot}H^+$, NO_2^+, and $C_2H_5OH{\cdot}H^+$ on the *E*/*N* ratios is similar to that in the case of the methyl nitrate (Table 1), the mechanisms of formation of NO_2^+ and $C_2H_5OH{\cdot}H^+$ ions are probably the same as those of the corresponding ions in the case of methyl nitrate. Indeed, the BE of $C_2H_5OH{\cdot}NO_2^+$ complex has been reported

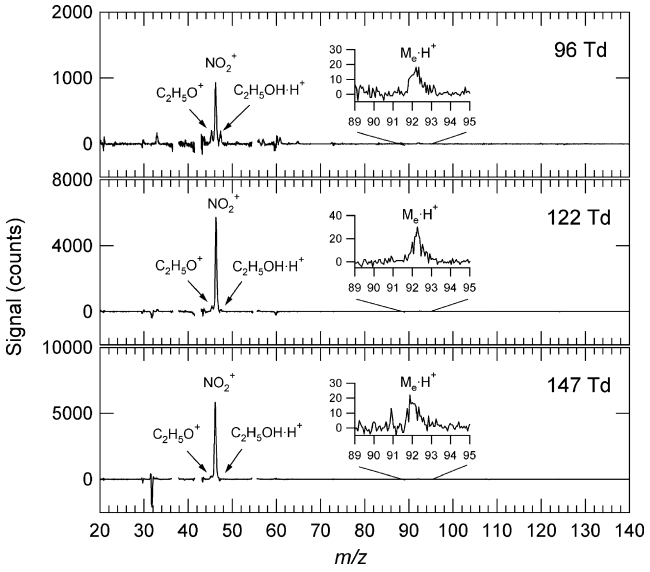

Fig. 4. Mass spectra of ethyl nitrate at three different *E*/*N* conditions.

to be $93 \pm 8\ kJ\ mol^{-1}$, which is similar to that of $CH_3OH{\cdot}NO_2^+$ complex [25].

$$C_2H_5ONO_2 + H_3O^+ \rightarrow M_e{\cdot}H^+ + H_2O \quad (10)$$

$$C_2H_5ONO_2 + H_3O^+ \rightarrow C_2H_5OH{\cdot}NO_2^+ + H_2O \quad (10a)$$

$$C_2H_5OH{\cdot}NO_2^+ \rightarrow C_2H_5OH + NO_2^+ \quad (11a)$$

$$C_2H_5ONO_2 + H_3O^+{\cdot}(H_2O)_{n=1,2} \rightarrow C_2H_5OH{\cdot}H^+ + HNO_3 + nH_2O \quad (12)$$

In addition to these ion peaks, a peak was identified at *m*/*z* 45 and assigned to $C_2H_5O^+$. The $C_2H_5O^+$ fragment was observed by the collisionally activated dissociation spectrometry of $C_2H_5OH{\cdot}NO_2^+$ and was assigned not to the ethoxy cation, but to CH_3CHOH^+ formed via a cyclic transition state [25].

$$C_2H_5OH{\cdot}NO_2^+ \rightarrow CH_3CHOH^+ + HONO \quad (11b)$$

The heat of formation of CH_3CHOH^+ has been reported to be $\leq 609\ kJ\ mol^{-1}$ [33], so that the reaction (11b) is an exothermic reaction with $\Delta H^\circ_{rxn} \leq -97\ kJ\ mol^{-1}$. However, reaction (11b) may involve a higher energy barrier than the BE of $C_2H_5OH{\cdot}NO_2^+$, because the production of CH_3CHOH^+ is minor compared with that of NO_2^+.

3.4. Mass spectra of n-propyl and isopropyl nitrates

Mass spectra of *n*-propyl and isopropyl nitrates are shown in Figs. 5 and 6, respectively. In both cases, ions of the protonated propyl nitrate ($M_{pr}{\cdot}H^+$), NO_2^+, and $C_3H_7O^+$ are detected at *m*/*z* 106, 46, and 59, respectively. The NO_2^+, and $C_3H_7O^+$ are probably formed by the same mechanisms as in the case of ethyl nitrate.

$$C_3H_7ONO_2 + H_3O^+ \rightarrow M_{pr}{\cdot}H^+ + H_2O \quad (13)$$

$$C_3H_7ONO_2 + H_3O^+ \rightarrow C_3H_7OH{\cdot}NO_2^+ + H_2O \quad (13a)$$

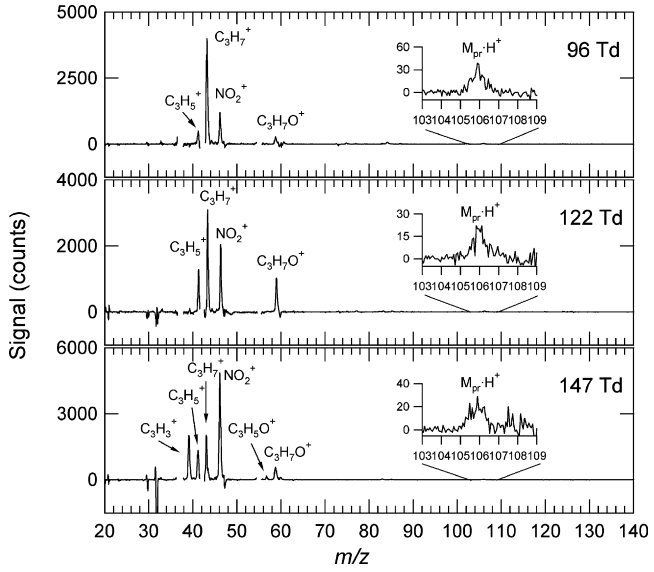

Fig. 5. Mass spectra of *n*-propyl nitrate at three different *E*/*N* conditions.

$$C_3H_7OH{\cdot}NO_2{}^+ \rightarrow C_3H_7OH + NO_2{}^+ \quad (14a)$$

$$C_3H_7OH{\cdot}NO_2{}^+ \rightarrow C_3H_7O^+ + HONO \quad (14b)$$

These peaks are relatively weak compared with the ion signals at *m*/*z* 43 at the low *E*/*N* condition. The peak at *m*/*z* 43 is assigned to $C_3H_7{}^+$. Several mechanisms for the formation of $C_3H_7{}^+$ are possible. One of these involves the possible formation of $C_3H_7{}^+$ by elimination of H_2O from $C_3H_7OH{\cdot}H^+$ [34], generated by the reaction of $C_3H_7ONO_2$ with $H_3O^+{\cdot}(H_2O)_{n=1,2}$ clusters, but this should be a minor process.

$$C_3H_7ONO_2 + H_3O^+{\cdot}(H_2O)_{n=1,2} \rightarrow C_3H_7OH{\cdot}H^+ + HNO_3 + nH_2O \quad (15)$$

$$C_3H_7OH{\cdot}H^+ \rightarrow C_3H_7{}^+ + H_2O \quad (16)$$

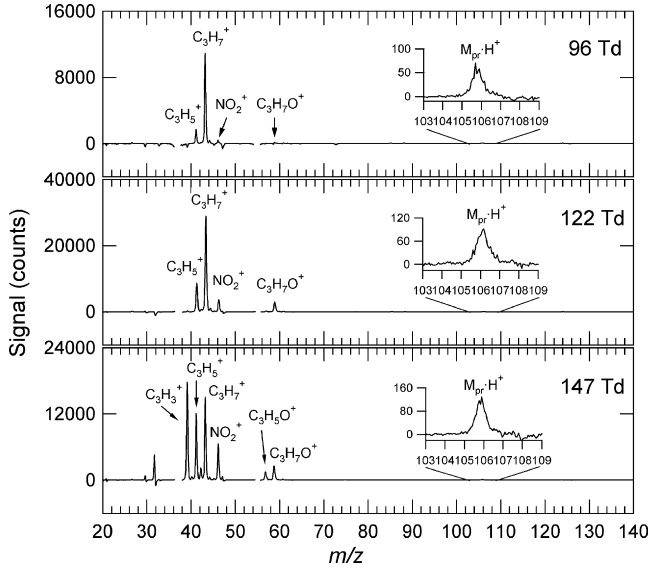

Fig. 6. Mass spectra of isopropyl nitrate at three different *E*/*N* conditions.

Another possible mechanism is the reaction of protonated propyl nitrate with H_2O in the drift tube to produce $C_3H_7OH{\cdot}H^+$, which eliminates H_2O [34].

$$M_{pr}{\cdot}H^+ + H_2O \rightarrow C_3H_7OH{\cdot}H^+ + HNO_3 \quad (17)$$

$$C_3H_7OH{\cdot}H^+ \rightarrow C_3H_7{}^+ + H_2O \quad (16)$$

The reaction (17) is likely to be exothermic: the ΔH°_{rxn} for the reaction (17) is estimated to be ≥ -11 for *n*-propyl nitrate and $\geq -15\,kJ\,mol^{-1}$ for isopropyl nitrate, assuming that the PAs of propyl nitrates are higher than that of ethyl nitrate [24,25]. In the estimation, the heats of formation used for *n*-propyl and isopropyl nitrates were -178 and $-197\,kJ\,mol^{-1}$, respectively; these values were calculated by Benson's group additivity methods [35]. Reactions similar to reaction (17) have been proposed in the case of peroxyacy nitrates from selected ion flow drift tube (SIFDT) experiments by Hansel and Wisthaler [17]. The direct formation of $C_3H_7{}^+$ by the CID of protonated propyl nitrates may be possible, since ionization potentials of *n*-propyl and isopropyl radicals are markedly lower than those of NO_2, *n*- and *i*-C_3H_7OH, and HNO_3 [24].

$$C_3H_7ONO_2 + H_3O^+ \rightarrow M_{pr}{\cdot}H^+ + H_2O \quad (13)$$

$$M_{pr}{\cdot}H^+ \rightarrow C_3H_7{}^+ + HNO_3 \quad (14c)$$

The ΔH°_{rxn} for reaction (14c) is estimated to be ≥ 142 for *n*-propyl nitrate and $\geq 80\,kJ\,mol^{-1}$ for isopropyl nitrate, which may be close to the BE of $C_3H_7OH{\cdot}NO_2{}^+$.

$C_3H_5{}^+$ ions at *m*/*z* 41 may be formed by the elimination of two hydrogen atoms from $C_3H_7{}^+$ as a result of collisions, even at the low *E*/*N* condition.

$$C_3H_7{}^+ \rightarrow C_3H_5{}^+ + H_2 \quad (18)$$

At *E*/*N* = 147 Td, the signals from $C_3H_3{}^+$ at *m*/*z* 39 and $C_3H_5O^+$ ions at *m*/*z* 57, which are probably formed by the elimination of two hydrogen atoms from $C_3H_5{}^+$ and $C_3H_7O^+$, respectively, become stronger.

3.5. Mass spectra of n-butyl and isobutyl nitrates

Mass spectra of *n*-butyl and isobutyl nitrates are shown in Figs. 7 and 8, respectively. Like the cases of propyl nitrates, ion signals of the protonated butyl nitrate ($M_b{\cdot}H^+$), $NO_2{}^+$, $C_4H_9O^+$, and $C_4H_9{}^+$ are observed at *m*/*z* 120, 46, 73, and 57, respectively, although the protonated *n*-butyl nitrate is not clearly detected compared with the protonated isobutyl nitrate. Ion signals of $C_4H_9{}^+$ are the most intense among the ion peaks in the mass spectra of both butyl nitrates under all *E*/*N* conditions.

$$C_4H_9ONO_2 + H_3O^+ \rightarrow M_b{\cdot}H^+ + H_2O \quad (19)$$

$$C_4H_9ONO_2 + H_3O^+ \rightarrow C_4H_9OH{\cdot}NO_2{}^+ + H_2O \quad (19a)$$

$$C_4H_9OH{\cdot}NO_2{}^+ \rightarrow C_4H_9OH + NO_2{}^+ \quad (20a)$$

$$C_4H_9OH{\cdot}NO_2{}^+ \rightarrow C_4H_9O^+ + HONO \quad (20b)$$

$$M_b{\cdot}H^+ + H_2O \rightarrow C_4H_9OH{\cdot}H^+ + HNO_3 \rightarrow C_4H_9{}^+ \quad (21)$$

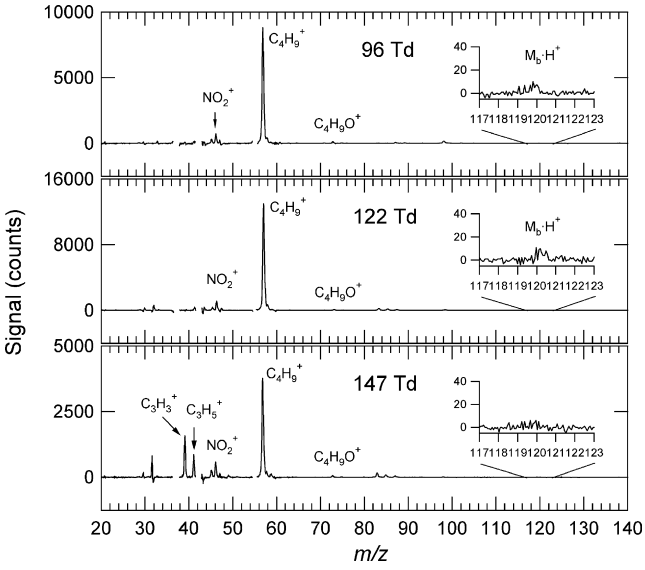

Fig. 7. Mass spectra of *n*-butyl nitrate at three different *E*/*N* conditions.

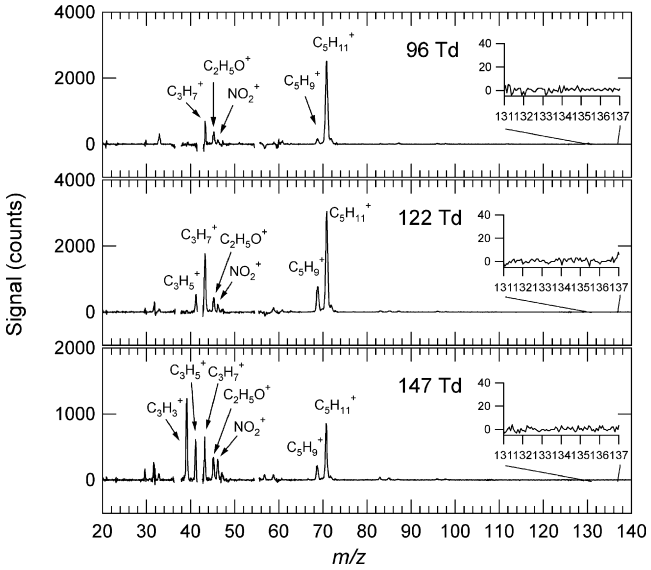

Fig. 9. Mass spectra of *n*-pentyl nitrate at three different *E*/*N* conditions.

and/or

$$M_b{\cdot}H^+ \rightarrow\ C_4H_9{}^+ + HNO_3 \qquad (20c)$$

At *E*/*N* = 147 Td, the signals from $C_3H_5{}^+$ and $C_3H_3{}^+$ ions at *m*/*z* 41 and 39, respectively, are strongly observed; these are probably fragment ions of $C_4H_9{}^+$. Ion signals observed at *m*/*z* 59 for isobutyl nitrate (Fig. 8) but not for *n*-butyl nitrate (Fig. 7) increased with increasing *E*/*N* ratio, so that these probably originate from some $C_3H_7O^+$ fragment.

3.6. Mass spectrum of n-pentyl nitrate

Mass spectra of *n*-pentyl nitrate are shown in Fig. 9. We did not observe ion signals of the protonated pentyl nitrate ($M_{pe}{\cdot}H^+$), at *m*/*z* 134, as shown in the mass spectra inserted in Fig. 9. Only *n*-$C_5H_{11}{}^+$ (*m*/*z* 71) is observed as a strong peak under all *E*/*N* conditions. $NO_2{}^+$ (*m*/*z* 46) and other organic fragment ions such as $C_5H_9{}^+$ (*m*/*z* 69), $C_2H_5O^+$ (*m*/*z* 45), $C_3H_7{}^+$ (*m*/*z* 43), $C_3H_5{}^+$ (*m*/*z* 41), and $C_3H_3{}^+$ (*m*/*z* 39) are weakly detected at the lower *E*/*N* values, and the intensities of these peaks increase at higher *E*/*N* values (see Table 1). The formation mechanism of *n*-$C_5H_{11}{}^+$ is probably:

$$n\text{-}C_5H_{11}ONO_2 + H_3O^+ \rightarrow\ M_{pe}{\cdot}H^+ + H_2O \qquad (22)$$

$$M_{pe}{\cdot}H^+ + H_2O\ \rightarrow n\text{-}C_5H_{11}OH{\cdot}H^+ + HNO_3 \rightarrow n\text{-}C_5H_{11}{}^+ \qquad (23)$$

and/or

$$M_{pe}{\cdot}H^+ \rightarrow n\text{-}C_5H_{11}{}^+ + HNO_3 \qquad (24)$$

For $NO_2{}^+$,

$$n\text{-}C_5H_{11}ONO_2 + H_3O^+ \rightarrow n\text{-}C_5H_{11}OH{\cdot}NO_2{}^+ + H_2O \qquad (22a)$$

$$n\text{-}C_5H_{11}OH{\cdot}NO_2{}^+ \rightarrow n\text{-}C_5H_{11}OH\ +\ NO_2{}^+ \qquad (25)$$

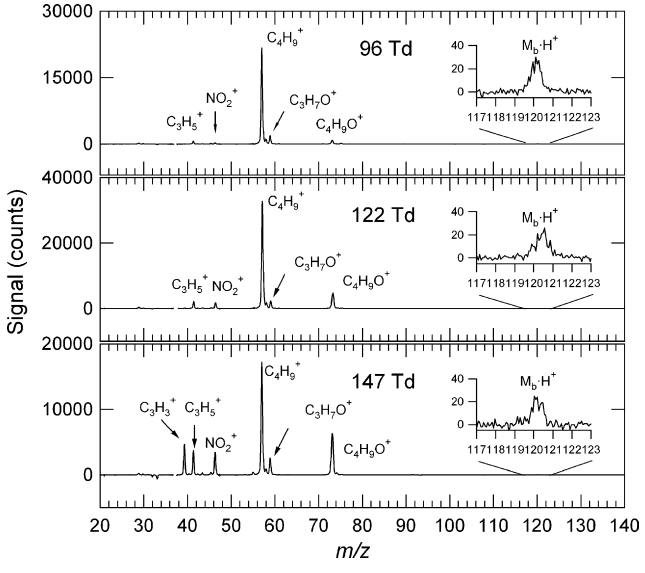

Fig. 8. Mass spectra of isobutyl nitrate at three different *E*/*N* conditions.

4. Discussion

The product ions and their fractional contribution to the total ion signals at the PTR ionization for seven C_1–C_5 alkyl nitrates ($RONO_2$, M) are summarized in Table 1. The ion signals of protonated alkyl nitrates, $M{\cdot}H^+$, are observed for C_1–C_4 alkyl nitrates. However, the signal intensities for these $M{\cdot}H^+$ ions are, at most, a few percent of those of the total ion signals in the *E*/*N* range examined (100–150 Td). This suggests that considerable fragmentation occurs, even at *E*/*N* = 100 Td. As shown in Table 1, the ion signals of $M{\cdot}H^+$ decrease and the contribution of the ion signals from fragment ions increases with increasing *E*/*N* ratio. Fragment ions such as $NO_2{}^+$ and RO^+ are probably produced by the CID of protonated alkyl nitrates $(ROH{\cdot}NO_2)^+$, where the protonation occurs at the RO group of $RONO_2$. For C_3–C_5 alkyl nitrates, R^+ ions may be produced by the reactions of $M{\cdot}H^+$ with H_2O followed by the elimination of H_2O from the resulting $ROH{\cdot}H^+$ ions and/or directly by the CID of $M{\cdot}H^+$.

For C_1–C_2 alkyl nitrates, small signals of $ROH{\cdot}H^+$ ions were observed, which were probably produced by the reactions of alkyl nitrates with $H_3O^+{\cdot}(H_2O)_{n=1,2}$ clusters. Processes for the formation of these fragment ions are summarized as follows:

$$RONO_2 + H_3O^+ \rightarrow M{\cdot}H^+ + H_2O \quad (26)$$

$$RONO_2 + H_3O^+ \rightarrow ROH{\cdot}NO_2{}^+ + H_2O \quad (26a)$$

$$ROH{\cdot}NO_2{}^+ \rightarrow ROH + NO_2{}^+ \quad (27a)$$

$$ROH{\cdot}NO_2{}^+ \rightarrow RO^+ + HONO \quad (27b)$$

$$M{\cdot}H^+ + H_2O \rightarrow ROH{\cdot}H^+ + HNO_3 \rightarrow R^+ + H_2O + HNO_3 \quad (28)$$

$$M{\cdot}H^+ \rightarrow R^+ + HNO_3 \quad (29)$$

$$RONO_2 + H_3O^+{\cdot}(H_2O)_{n=1,2} \rightarrow ROH{\cdot}H^+ + HNO_3 + nH_2O \quad (30)$$

For C_1–C_2 alkyl nitrates, the ion signals of $NO_2{}^+$ predominate, whereas the ion signals of R^+ predominate for C_3–C_5 alkyl nitrates. At high *E*/*N* conditions (147 Td), the mass spectrum of alkyl nitrates becomes more complicated because of the increasing complexity of fragmentation processes that form $[R-2H]^+$, $[R-4H]^+$, $[RO-2H]^+$, etc., particularly in the case of higher alkyl nitrates.

The approximate relative intensities of product ions from alkyl nitrates with reference to the intensity of $CH_3CN{\cdot}H^+$ at *m*/*z* 42, obtained when pure acetonitrile was injected, are listed in Table 2. These values correspond to the relative detection sensitivity of ions referenced to acetonitrile. The normalized detection sensitivity of acetonitrile was approximately 90 [normalized counts (ncounts)]/[part per billion by volume (ppbv)] normalized to the total $H_3O^+{\cdot}(H_2O)_{n=0,1,2}$ intensity of 10^6 counts under all *E*/*N* conditions. The *m*/*z* of protonated alkyl nitrates is useful in easily discriminating C_1–C_4 alkyl nitrates from other VOCs; however, the detection sensitivity of those ion peaks is at least three orders of magnitude less than that of acetonitrile. For C_1–C_2 alkyl nitrates, the most intense peak is that of $NO_2{}^+$, for which the detection sensitivity significantly increases with increasing *E*/*N* ratio. The ion intensity of $NO_2{}^+$ for methyl nitrate become comparable to that of acetonitrile at *E*/*N* = 122 and 147 Td, whereas the ion intensity of $NO_2{}^+$ for ethyl nitrate is 5- to 25-fold less than that of acetonitrile. Because most organic nitrates would give $NO_2{}^+$ ions (Table 1), the detection of the $NO_2{}^+$ ions is not selective for C_1–C_2 alkyl nitrates. For C_3–C_5 alkyl nitrates, the detection sensitivity of R^+ ions, the signals of which are among the more intense of those of detected ions, is 5- to 20-fold less than that of acetonitrile at *E*/*N* = 96 Td.

The product ions, $M{\cdot}H^+$, R^+, $ROH{\cdot}H^+$, and RO^+, obtained in the present work are equivalent to MH^+, $[MH-HNO_3]^+$, $[MH+H_2O-HNO_3]^+$, and $[MH-HNO_2]^+$, respectively, for *n*-propyl and *n*-butyl nitrates reported by D'Anna et al. [12],

Table 2
Estimated relative ion intensities of product ions referenced to acetonitrile

	$M{\cdot}H^+$	$NO_2{}^+$	RO^+	R^+	$ROH{\cdot}H^+$	Other product ions	Total
Acetonitrile	100						100
E/*N* = 96 Td ($CH_3CN{\cdot}H^+$: 4.5×10^5 ncounts)[a]							
$RONO_2$							
R═CH_3	0.5	21	–	–	2		24
C_2H_5	<0.1	3	0.7	–	0.6		4
n-C_3H_7	<0.1	4	0.8	13	–	1 ($C_3H_5{}^+$)	19
i-C_3H_7	0.1	0.4	0.1	12	–	2 ($C_3H_5{}^+$)	15
n-C_4H_9	<0.1	1	0.2	17	–		18
i-C_4H_9	<0.1	0.1	0.6	14	–	1 ($C_3H_7O^+$)	16
n-C_5H_{11}	–	0.2	–	6	–	0.3 ($C_5H_9{}^+$)	7
E/*N* = 122 Td ($CH_3CN{\cdot}H^+$: 4.6×10^5 ncounts)[a]							
R═CH_3	0.6	80	–	–	0.6		81
C_2H_5	<0.1	15	0.9	–	0.3		16
n-C_3H_7	<0.1	3	2	5	–	2 ($C_3H_5{}^+$)	12
i-C_3H_7	0.1	2	2	19	–	0.1 ($C_3H_5{}^+$)	23
n-C_4H_9	<0.1	1	0.1	18	–		19
i-C_4H_9	<0.1	0.9	3	17	–	1 ($C_3H_7O^+$)	22
n-C_5H_{11}	–	0.2	–	4	–	1 ($C_5H_9{}^+$)	5
E/*N* = 147 Td ($CH_3CN{\cdot}H^+$: 4.2×10^5 ncounts)[a]							
R═CH_3	0.7	126	–	–	0.5		127
C_2H_5	<0.1	22	0.9	–	–		23
n-C_3H_7	<0.1	15	2	6	–	5 ($C_3H_5{}^+$), 7 ($C_3H_3{}^+$), 0.5 ($C_3H_5O^+$)	36
i-C_3H_7	0.1	5	2	12	–	9 ($C_3H_5{}^+$), 15 ($C_3H_3{}^+$), 1 ($C_3H_5O^+$)	44
n-C_4H_9	<0.1	1	0.1	7	–	1 ($C_3H_5{}^+$)	9
i-C_4H_9	<0.1	2	5	11	–	2 ($C_3H_7O^+$), 2 ($C_3H_5{}^+$)	22
n-C_5H_{11}	–	0.5	–	1	–	0.8 ($C_3H_5{}^+$), 2 ($C_3H_3{}^+$), 0.5 ($C_2H_5O^+$), 0.4 ($C_5H_9{}^+$)	5

[a] The ncounts (normalized counts) show ion counts normalized to the total $H_3O^+{\cdot}(H_2O)_{n=0,1,2}$ intensity of 10^6 counts.

who used a commercial PTR-MS instrument operated at $E/N \approx 80$ Td. The product ions, their relative signal abundances, and their sensitivity were reported in the case of *n*-butyl nitrate. Ion signals at *m/z* 29, 57, and 75 were observed with relative intensities of 13:100:10, and the normalized sensitivity was 24.4 [normalized counts per second (ncps)]/ppbv normalized to a total $H_3O^+ \cdot (H_2O)_{n=0,1,2}$ intensity of 10^6 cps. The ion signals predominantly observed at *m/z* 57 should be attributed to *n*-$C_4H_9^+$, which is consistent with the results obtained in the present work. The ion signals at *m/z* 75 might be assigned to *n*-$C_4H_9OH \cdot H^+$, which were not observed under the lowest *E/N* condition (96 Td) used in the present work. The difference is probably a result of the different *E/N* conditions. The ion signals at *m/z* 29 were not observed, even at a higher *E/N* condition (147 Td) in the present work, suggesting that the product that D'Anna et al. synthesized included some impurities that produced $C_2H_5^+$ and/or HCO^+ at a significant level. Here, the values of normalized sensitivity obtained by the PTR-TOFMS (ncounts/ppbv) were directly compared with those obtained by PTR-MS (ncps/ppbv), assuming that the duty cycle of TOFMS was constant in the *m/z* range of interest. The present normalized sensitivity of *n*-butyl nitrate was estimated to be 15 ncounts/ppbv at $E/N = 96$ Td by using the peak at *n*-$C_4H_9^+$, which is comparable to the normalized sensitivity of 20 ncps/ppbv estimated by D'Anna et al. using the same peak. However, the relative sensitivity of *n*-butyl nitrate referenced to typical VOCs such as acetonitrile and acetone, is different from the present one [15 ncounts/ppbv versus 90 ncounts/ppbv (for acetonitrile)] and from the result by D'Anna et al. [20 ncps/ppbv versus 38 ncps/ppbv (for acetone)], although the normalized sensitivities of acetonitrile and acetone were similar [7,15]. This is probably caused by differences in the amount of water vapor in the drift tube. Since the PAs of alkyl nitrates are expected to be close to that of H_2O, the detection sensitivities could be influenced considerably by the amount of water vapor in the drift tube [21].

Mass spectra of methyl, ethyl, *n*-pentyl, and isopentyl nitrates obtained by chemical ionization mass spectrometry using methane (CH_4) as the reagent gas have been reported [36–38]. The reagent ions produced in an ion source were mainly CH_5^+ and $C_2H_5^+$. The ion signals of the protonated methyl and ethyl nitrates formed by PTR ionization from CH_5^+ [$PA(CH_4) = 544$ kJ mol^{-1}] and $C_2H_5^+$ [$PA(C_2H_4) = 681$ kJ mol^{-1}] [24] were strong compared with those of fragment ions such as NO_2^+. Ratios of ion signals of $RONO_2 \cdot H^+$ to those of NO_2^+ are approximately 10:1 and 2:1 for methyl and ethyl nitrates [36], respectively, resulting in mass spectral patterns that are quite different to the present ones (Figs. 3 and 4). This is mainly the result of differences in the kinetic energies in the ionization region: the presence of H_2O in the ionization region would also have some effect on the mass patterns of alkyl nitrates. Ion signals of protonated *n*-pentyl and isopentyl nitrates were not observed when detecting *n*-pentyl and isopentyl nitrates [36]. The fragment ions were observed only at *m/z* 46, 57, 69, 71, 72, 85, 87, and 132. The ion signals at *m/z* 71 were the most intense, which is consistent with the present findings for *n*-pentyl nitrate.

5. Concluding remarks

Mass spectra of C_1–C_5 alkyl nitrates ($RONO_2$) were recorded by using a custom-built PTR-TOFMS instrument. PTR-MS detection of alkyl nitrates has the potential for detecting the protonated parent molecules in the case of smaller C_1–C_4 alkyl nitrates, but their ion counts are quite small and fragmentation processes, which produce, NO_2^+, RO^+, R^+, and $ROH \cdot H^+$ ions, occur to a considerable extent following PTR ionization of the alkyl nitrates. For larger alkyl nitrates, the detection of the protonated alkyl nitrates is not possible, as a result of fragmentation reactions; ion signals of R^+ are, however, detected. The detection sensitivity is estimated to be 5- to 20-fold less than that of acetonitrile, a typical VOC, on the basis of the abundance of R^+ ions. This suggests that these fragment ions sometimes overlap with protonated alkenes in PTR ionization, and that attention should be paid to the ion signals of protonated alkenes, particularly when VOCs and $RONO_2$ are mixed. Measurements of thermally decomposed air samples help to identify the origins of the product ion signals and permit protonated alkenes ($alkene \cdot H^+$) to be distinguished from R^+ fragments from alkyl nitrates.

Acknowledgements

The authors are grateful to an anonymous reviewer for helpful suggestions and comments in improving the manuscript. We are also grateful Jun Hirokawa (Hokkaido University) and Kei Sato (NIES) for their valuable comments. This work was financially supported by the Ministry of the Environment through the Environmental Technology Development Fund (FY 2004–2005), and partly by the Steel Industry Foundation for the Advancement of Environmental Protection Technology (FY 2005-2006).

References

[1] W. Lindinger, A. Hansel, A. Jordan, Int. J. Mass Spectrom. Ion Process. 173 (1998) 191.
[2] W. Lindinger, A. Hansel, A. Jordan, Chem. Soc. Rev. 27 (1998) 347.
[3] A. Hansel, A. Jordan, C. Warneke, R. Holzinger, W. Lindinger, Rapid Commun. Mass Spectrom. 12 (1998) 871.
[4] T. Karl, P.J. Crutzen, M. Mandl, M. Staudinger, A. Guenther, A. Jordan, R. Fall, W. Lindinger, Atmos. Environ. 35 (2001) 5287.
[5] T. Karl, A. Hansel, T. Märk, W. Lindinger, D. Hoffmann, Int. J. Mass Spectrom. 223 (2003) 527.
[6] T. Karl, T. Jobson, W.C. Kuster, E. Williams, J. Stutz, R. Shetter, S.R. Hall, P. Goldan, F. Fehsenfeld, W. Lindinger, J. Geophys. Res. 108 (2003) 4508, doi:10.1029/2002JD003333.
[7] J.A. de Gouw, P.D. Goldan, C. Warneke, W.C. Kuster, J.M. Roberts, M. Marchewka, S.B. Bertman, A.A.P. Pszenny, W.C. Keene, J. Geophys. Res. 108 (2003) 4682, doi:10.1029/2003JD003863.
[8] R. Holzinger, C. Warneke, A. Hansel, A. Jordan, W. Lindinger, D.H. Scharffe, G. Schade, P.J. Crutzen, Geophys. Res. Lett. 26 (1999) 1161.
[9] T. Karl, A. Guenther, A. Jordan, R. Fall, W. Lindinger, Atmos. Environ. 35 (2001) 491.
[10] W. Grabmer, M. Graus, C. Lindinger, A. Wisthaler, B. Rappenglück, R. Steinbrecher, A. Hansel, Int. J. Mass Spectrom. 239 (2004) 111.
[11] C. Spirig, A. Neftel, C. Ammann, J. Dommen, W. Grabmer, A. Thielmann, A. Schaub, J. Beauchamp, A. Wisthaler, A. Hansel, Atmos. Chem. Phys. 5 (2005) 465.

[12] B. D'Anna, A. Wisthaler, Ø. Andreasen, A. Hansel, J. Hjorth, N.R. Jensen, C.J. Nielsen, Y. Stenstrøm, J. Viidanoja, J. Phys. Chem. A 109 (2005) 5104.
[13] D. Paulsen, J. Dommen, M. Kalberer, A.S.H. Prévôt, R. Richter, M. Sax, M. Steinbacher, E. Weingartner, U. Baltensperger, Environ. Sci. Technol. 39 (2005) 2668.
[14] A. Lee, A.H. Goldstein, M.D. Keywood, S. Gao, V. Varutbangkul, R. Bahreini, N.L. Ng, R.C. Flagan, J.H. Seinfeld, J. Geophys. Res. 111 (2006), doi:10.1029/2005JD006437, D07302.
[15] C. Warneke, J. de Gouw, W.C. Kuster, P.D. Goldan, R. Fall, Environ. Sci. Technol. 37 (2003) 2494.
[16] J.M. Roberts, Atmos. Environ. 24A (1990) 243.
[17] A. Hansel, A. Wisthaler, Geophys. Res. Lett. 27 (2000) 895.
[18] R. Atkinson, Atmos. Environ. 34 (2000) 2063.
[19] R.S. Rosen, E.C. Wood, P.J. Wooldridge, J.A. Thornton, D.A. Day, W. Kuster, E.J. Williams, B.T. Jobson, R.C. Cohen, J. Geophys. Res. 109 (2004), doi:10.1029/2003JD004227, D07303.
[20] S. Inomata, H. Tanimoto, N. Aoki, J. Hirokawa, Y. Sadanaga, Rapid Commun. Mass Spectrom. 20 (2006) 1025.
[21] H. Tanimoto, N. Aoki, S. Inomata, J. Hirokawa, Y. Sadanaga, Int. J. Mass Spectrom 263 (2007) 1, doi:10.1016/j.ijms.2007.01.009.
[22] A.P. Black, F.H. Babers, in: A.H. Blatt (Ed.), Organic Synthesis, Collective, vol. 2, John Wiley & Sons, Inc., New York, 1943, p. 412.
[23] A.F. Ferris, K.W. McLean, I.G. Marks, W.D. Emmons, J. Am. Chem. Soc. 75 (1953) 4087.
[24] W.G. Mallard (Ed.), NIST Chemistry WebBook, NIST Standard Reference Database Number 69, National Institute of Standards and Technology, Gaithersburg, MD, 2005 (http://webbook.nist.gov).
[25] M. Aschi, F. Cacace, G. de Petris, F. Pepi, J. Phys. Chem. 100 (1996) 16522.
[26] G.D. Mendenhall, D.M. Golden, S.W. Benson, Int. J. Chem. Kinet. 7 (1975) 725.
[27] D.A. Day, P.J. Wooldridge, M.B. Dillon, J.A. Thornton, R.C. Cohen, J. Geophys. Res. 107 (2002) 4046.
[28] H.J. Curran, Int. J. Chem. Kinet. 38 (2006) 250.
[29] R. Atkinson, D.L. Baulch, R.A. Cox, R.F. Hampson Jr., J.A. Kerr, M.J. Rossi, J. Troe, J. Phys. Chem. Ref. Data 26 (1997) 521.
[30] T.J. Lee, J.E. Rice, J. Am. Chem. Soc. 114 (1992) 8247.
[31] M. Polášek, F. Tureček, J. Am. Soc. Mass Spectrom. 11 (2000) 380.
[32] L.S. Sunderlin, R.R. Squires, Chem. Phys. Lett. 212 (1993) 307.
[33] B. Ruscic, J. Berkowitz, J. Chem. Phys. 101 (1994) 10936.
[34] P. Spanel, D. Smith, Int. J. Mass. Spectrom. Ion Processes 167/168 (1997) 375.
[35] S.W. Benson, Thermochemical Kinetics, 2nd ed., John Wiley & Sons, Inc., New York, 1976, 19–77.
[36] R.C. Das, O. Koga, S. Suzuki, Bull. Chem. Soc. Jpn. 52 (1979) 65.
[37] M. Attinà, F. Cacace, M. Yañez, J. Am. Chem. Soc. 109 (1987) 5092.
[38] J. Kames, U. Schurath, F. Flocke, A. Volz-Thomas, J. Atmos. Chem. 16 (1993) 349.